

# Paper-Based Coculture Platform to Evaluate the Effects of Fibroblasts on Estrogen Signaling in ER+ Breast Cancers

Zachary R. Sitte,<sup>§</sup> Abel Andre Miranda Buzetta,<sup>§</sup> Sarina J. Jones,<sup>§</sup> Zhi-Wei Lin, Nathan Ashbrook Whitman, and Matthew R. Lockett\*



Cite This: *ACS Meas. Sci. Au* 2023, 3, 479–487



Read Online

ACCESS |



Metrics & More



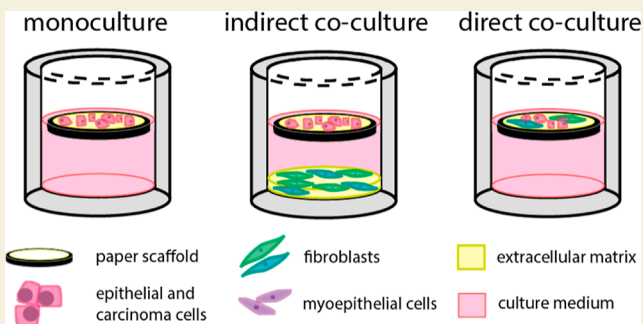
Article Recommendations



Supporting Information

**ABSTRACT:** Cell-based assays enable molecular-level studies of cellular responses to drug candidates or potential toxins. Transactivation assays quantify the activation or inhibition of nuclear receptors, key transcriptional regulators of gene targets in mammalian cells. One such assay couples the expression of luciferase to the transcriptional activity of estrogen receptor- $\alpha$  (ER $\alpha$ ). While this assay is regularly used to screen for agonists and antagonists of the estrogen signaling pathway, the setup relies on monolayer cultures in which cells are plated directly onto the surface of cell-compatible plasticware. The tumor microenvironment is more than a collection of cancerous cells and is profoundly influenced by tissue architecture, the presence of extracellular matrices, and intercellular signaling molecules produced by non-cancerous neighboring cells (e.g., fibroblasts). There exists a need for three-dimensional culture platforms that can be rapidly prototyped to assess new configurations and readily produced in the large numbers needed for translational studies and screening applications. Here, we demonstrate the utility of the paper-based culture platform to probe the effects of intercellular signaling between two cell types. We used paper scaffolds to generate tumor-like environments, forming a defined volume of breast cancer cells suspended in collagen. By placing the paper scaffolds in commercial 96-well plates, we compared monocultures of only breast cancer cells with coculture configurations containing fibroblasts in different locations that mimicked the stages of breast cancer progression. We show that ER $\alpha$  transactivation in the T47D-KBluc cell line is affected by the presence, number, and proximity of fibroblasts, and is a consequence of intercellular signaling molecules. After screening a small library of fibroblast-secreted signaling molecules, we showed that interleukin-6 (IL-6) was the primary driver of reduced estradiol sensitivity. These effects were mitigated in the coculture configurations by the addition of an IL-6 neutralizing antibody. We also assessed estrogen receptor expression and transcriptional regulation, further demonstrating the utility of the paper-based platform for detailed mechanistic studies.

**KEYWORDS:** cell-based assays, 3D culture, hormone signaling, paracrine signaling, cancer progression



## INTRODUCTION

Breast cancer is the most frequently diagnosed cancer in women worldwide, with an estimated 298,000 new cases in the United States in 2023.<sup>1,2</sup> Treatment decisions are based on the tumor's molecular subclass, which is defined by the presence of hormone receptors, including estrogen receptor- $\alpha$  (ER $\alpha$ ), human epidermal growth factor receptor 2 (HER2/neu), and progesterone receptor (PR).<sup>3</sup> Nearly 80% of breast cancer patients have estrogen-receptor-positive (ER+) tumors. These cancer cells require estrogenic molecules to initiate proliferation and invasion.<sup>4,5</sup> This hormone dependence is leveraged with adjuvant therapies that inhibit estrogen receptor activity, selectively degrade the receptor, or target the enzyme that synthesizes its natural agonist, 18-carbon estrogens.<sup>6</sup> The detection of ER $\alpha$  expression in patient samples does not guarantee treatment success as adjuvant hormone therapies have limited effectiveness against cells with de novo or

acquired resistance.<sup>7</sup> Acquired resistance is attributed to the tumor microenvironment, which includes surrounding stromal cell types, signaling molecules, and the supply of oxygen and nutrients. Soluble signaling molecules and growth factors secreted by the stromal cells may not decrease the expression of ER $\alpha$  but rather limit its activity through post-translational modifications of the receptor or by depleting the availability of coregulators needed for its transactivation.<sup>8,9</sup>

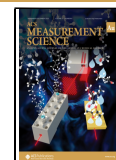
Much of our understanding of ER $\alpha$  signaling and regulation in human mammary epithelial tissues and breast carcinomas

**Received:** July 26, 2023

**Revised:** September 22, 2023

**Accepted:** September 25, 2023

**Published:** October 9, 2023



comes from monolayer cultures in which a single cell type is plated directly onto cell-compatible plasticware. These monolayer cultures are the standard for identifying endocrine disruptors and potential therapies. Transactivation assays often rely on end-point readouts, which quantify the ER $\alpha$  activity in the presence of agonists and antagonists through the expression of a reporter protein or enzyme.<sup>10</sup> There is a need for physiologically relevant tumor microenvironment models, which overcome the poor predictive power of current monolayer cell-based assays. By incorporating extracellular matrices and stromal components into these cell-based assays, aspects of the structural and signaling components affecting tumor progression are included. The extracellular matrix (ECM) maintains tissue structure and plays an important role in breast tissue development and homeostasis. Three-dimensional culture environments such as the collagen overlay or sandwich format pioneered by Bissell result in mammary epithelial cell polarization and casein production, phenotypes not found in monolayer cultures.<sup>11–13</sup> Signaling between breast epithelial cells and stromal components such as fibroblasts can also promote tumorigenesis.<sup>14</sup> Normal-associated or lobular fibroblasts are responsible for the development and branching of the luminal structures that serve as milk ducts.<sup>15</sup> Cancer-associated fibroblasts are morphologically and functionally distinct from normal fibroblasts and responsible for tumor growth and progression in the lumen.<sup>16</sup>

Stromal fibroblasts and adipocytes have been incorporated into three-dimensional (3D) culture formats, including mammosphere cultures, microfluidic devices, and bioprinted constructs.<sup>17–19</sup> Each of these setups has positive and negative aspects. Mammospheres are easily set up but are limited to microscopy or histology readouts as the different cell types are in contact. Microfluidic devices and bioprinted constructs can pattern different cell types, placing them in separate locations. These technologies have significant barriers to access for many tissue culture laboratories as they require engineering expertise and specialized equipment for assembly and maintenance. The paper-based culture platform first described by Whitesides<sup>20</sup> and advanced by our laboratory and others is ideal for the rapid prototyping and scale production of scaffolds that support cells in tissue-like environments. The paper serves as a preformed porous scaffold to which cell-laden gels are deposited in regions defined by wax-printed borders or precut shapes. The cellulose fibers of the paper support the thin cell-laden gels, which are otherwise too fragile to handle or manipulate.

We have used paper scaffolds to develop cell-based assays for quantifying cellular invasion,<sup>21–23</sup> evaluating the role of hypoxia on ER $\alpha$  expression and activity,<sup>24,25</sup> and characterizing drug permeation and metabolism in thick tumor-like structures.<sup>26,27</sup> Here, we expand on our previous work, focusing on cocultures containing estrogen receptor positive (ER+) carcinoma cell lines and normal mammary fibroblasts. Specifically, we compared ER $\alpha$  signaling in cocultures where fibroblasts were physically separated from or in direct contact with breast cancer cells. We quantified the effects of the presence, proximity, and number of mammary fibroblasts on the estrogen-dependent signaling in the ER+ T47D and MCF7 cell lines. We found that the presence and proximity of the fibroblasts to T47D cells decreased luciferase activity in our transactivation assay but did not inhibit the transcription activity of ER $\alpha$ . By removing the proinflammatory cytokine

interleukin-6 (IL-6) from the coculture configuration with neutralizing antibodies, transactivation in the presence of estradiol (E2) matched the monoculture configuration, further suggesting that the coculture inhibited the translation and activity of ER $\alpha$ -regulated genes.

## MATERIALS AND METHODS

### Reagents

All reagents were used as received unless otherwise noted. Human recombinant interleukin-6 (IL-6), interleukin-8 (IL-8), stromal-cell derived factor-1-alpha (SDF-1), transforming growth factor-beta-2 (TGF- $\beta$ ), and tumor necrosis factor-alpha (TNF- $\alpha$ ) were purchased from GenScript. Dimethyl sulfoxide, ethanol, and radioimmunoprecipitation assay (RIPA) buffer were purchased from Fisher Scientific. 17 $\beta$ -Estradiol (E2) and 4-hydroxytamoxifen (TAM) were purchased from Millipore Sigma. The CellTiter-Glo 2.0 Viability Assay (CTG), ONE-Glo Luciferase Assay, and Reporter Lysis 5 $\times$  buffer were purchased from Promega. Anti-IL-6 (MAB206) and anti-TNF- $\alpha$  (AF410NA) neutralizing antibodies were purchased from R&D Systems.

### Cell Culture and Maintenance

Cell culture medium and supplements were purchased from Gibco, except for collagen I (rat tail, Corning) and fetal bovine serum (FBS, VWR). The MCF7, MDA-MB-231 (M231), T47D, and T47D-KBluc cell lines were purchased from the American Type Culture Collection. Human reductive mammary fibroblasts (RMFs or normal fibroblasts) were generously provided by Charlotte Kupperwasser at the Tufts University School of Medicine. The characterization and use of these cells were detailed previously.<sup>28,29</sup> All cells were maintained as monolayers in phenol-red-free high-glucose Dulbecco's modified Eagle's medium at 37 °C, 5% CO<sub>2</sub>, and ambient oxygen tensions. The MCF7, M231, and T47D medium contained 10% FBS, 2 mM L-glutamine, 25 mM N-2-hydroxyethylpiperazine-N'-2-ethanesulfonic acid (HEPES), 1% PenStrep, and 1 mM sodium pyruvate. The RMF maintenance medium contained 10% FBS, 2 mM L-glutamine, 25 mM HEPES, 1% 1 $\times$  nonessential amino acids, 1% PenStrep, and 1 mM sodium pyruvate. The T47D-KBluc cell maintenance medium contained 10% FBS, 0.5 mg/mL geneticin, 0.05 mg/mL gentamicin, 2 mM L-glutamine, 25 mM HEPES, 1 $\times$  nonessential amino acids, and 1 mM sodium pyruvate. The culture medium was exchanged every 48 h, and the cells were passed at 80% confluency with TrypLE using standard procedures. Unless otherwise stated, the breast cancer cell lines were maintained for 3 d in a withdrawal medium containing 10% charcoal-stripped FBS and the appropriate supplements before use.

### 3D Culture Preparation

The paper scaffolds were prepared as detailed previously.<sup>30,31</sup> Sheets of Whatman 105 lens paper were wax patterned with a 3.0 mm diameter circle of exposed paper surrounded by a 1.5 mm wax border. Each pattern constituted a scaffold, which fit directly into a 96-well plate. Photographs and schematics of the paper scaffolds are in the Supporting Information. The scaffolds were deposited with 0.5  $\mu$ L of 1.2 mg/mL neutralized collagen I. Cell-free scaffolds contained only collagen. Cell-containing scaffolds contained 4.0  $\times$  10<sup>4</sup> breast cancer cells, for a final density of 4.0  $\times$  10<sup>7</sup> cells/cm<sup>3</sup>. The cell-laden collagen was prepared by pelleting the desired number of cells with centrifugation (1000 $\times$ g, 5 min) and thoroughly dispersing the pellet in the appropriate volume of collagen.

### Cellular Viability and ER Transactivation Assays

Cellular viability was measured with the CTG assay. Transactivation of luciferase in T47D-KBluc cells was measured with the ONE-Glo assay. After exposure to E2, the scaffolds were washed in 1 $\times$  PBS, submerged in a 1:4 (v/v) mixture of Reporter Lysis 5 $\times$  Buffer and 1 $\times$  PBS, and agitated for 10 min at room temperature. Aliquots of lysate (50  $\mu$ L) were transferred to a fresh 96-well plate and mixed with equal volumes of CTG or the OneGlo reagent. Luminescence values were recorded on a SpectraMax M5 plate reader (Molecular Devices).

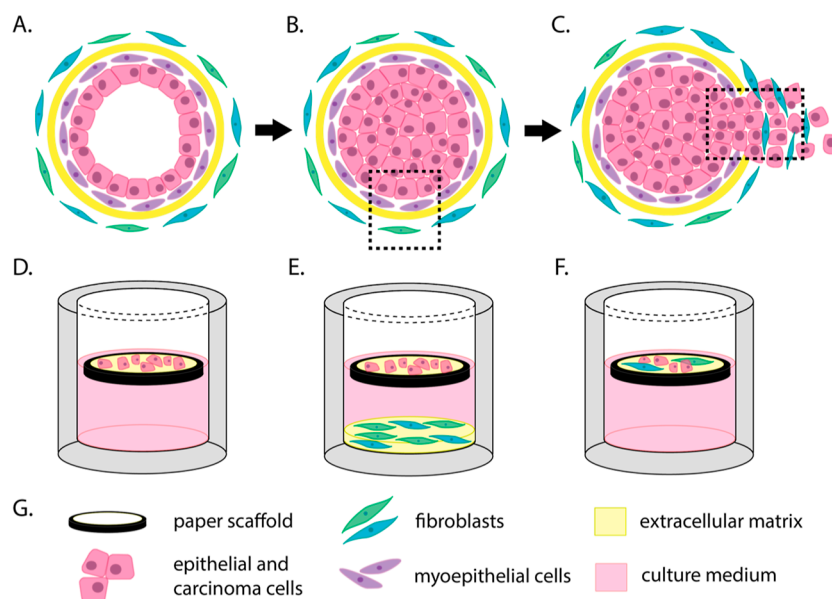


**Figure 1.** (A–C) Schematics of breast carcinoma progression. (A) Healthy lumen or milk duct defined by a proteinaceous ECM layer that separates the epithelial and stromal components. (B) Ductal carcinoma in situ or DCIS structure in which a solid tumor forms and fills the lumen. (C) Invasive ductal carcinoma or IDC structure in which the extracellular barrier is degraded and the epithelial and stromal components can freely intermingle. (D–F) Schematics of the three culture configurations used to mimic different aspects of breast cancer progression. The paper scaffolds remained at the air–water interface throughout each experiment in these configurations. (D) Monoculture configuration in which paper scaffolds containing breast cancer cell-laden collagen were placed in 96-well plates prefilled with culture medium. (E) Indirect coculture configuration, which mimics aspects of the DCIS structure highlighted by the box in part (B). This configuration was prepared by depositing fibroblast-laden collagen onto the bottom of a 96-well plate, filling the well with the culture medium, and placing a breast cancer cell-containing paper scaffold on top of the medium. (F) Direct coculture configuration, which mimics aspects of the IDC structure highlighted by the box in (C). This configuration was prepared by filling the well with culture medium and placing a paper scaffold containing both breast cancer cells and fibroblasts on top of the medium. (G) Legend of each component in the schematics. Myoepithelial cells are an important aspect of the lumen microenvironment and includes in the (A)–(C), but not one explored in the current culture configurations.

Estradiol stocks were prepared at 1000× the dosing concentration in ethanol and stored at 4 °C until needed.

### RNA Extraction and RT-qPCR

Each scaffold was submerged in TRIzol reagent and agitated for 5 min before ribonucleic acid (RNA) extraction with a PureLink RNA Mini Kit (Invitrogen), following the manufacturer's procedure. Isolated RNA (1 μg) was reverse transcribed with a High-Capacity Reverse Transcription Kit (ThermoFisher) in an Eppendorf MasterCycler. Table S1 lists each primer sequence, optimized primer concentrations, and reaction efficiencies. Amplification reactions were performed with a PowerUP SYBR Master Mix (ThermoFisher), in a 384-well plate, on a QuantStudio 6 Flex Real-Time polymerase chain reaction (PCR) system. Each gene was measured in quadruplicate with the following amplification program: 95 °C for 2 min, 40 cycles of 95 °C for 1 s, and 60 °C for 30 s. Each transcript was quantified with the  $\Delta\Delta C_t$  method against  $\beta$ -actin (*ACTB*) as the housekeeping gene.<sup>32</sup> Average  $\Delta\Delta C_t$  fold changes of  $\geq 2.0$  from assays prepared from three different cell passages (i.e., three biological replicates) were evaluated for significance by comparing the  $\Delta C_t$  values against the negative control.<sup>33</sup>

### Protein Quantification and Synthesis Measurements

Each scaffold was submerged in ice-cold RIPA buffer and agitated on an orbital shaker at 4 °C for 20 min. The lysate was clarified with centrifugation (10,000×g, 4 °C, 10 min), the protein was quantified with a Bicinchoninic Acid Protein assay, and the lysate was diluted accordingly in 1X PBS before quantification with an ER $\alpha$  enzyme-linked immunoassay (ELISA) kit (R&D Systems). Total protein synthesis in the monoculture configurations was measured with a Protein Synthesis Assay Kit (Cayman Chemical), following the manufacturer's protocol. In brief, 10,000 T47D-KBluc cells were incubated for 24 h in 200 μL of withdrawal medium containing 10 nM E2 and 100 ng/mL of IL-6, IL-8, TGF- $\beta$ , or TNF- $\alpha$ .

Cycloheximide (50 μg/mL) served as the positive control. The fluorescence intensity was measured on a SpectraMax MiniMax 300 imaging cytometer.

### Neutralizing Antibody Assays

Indirect coculture configurations containing  $4.0 \times 10^4$  T47D-KBluc cells and  $4.0 \times 10^4$  RMFs were exposed to 100 μL of withdrawal medium containing 10 nM E2 and neutralizing antibody for 24 h: 800 ng/mL anti-IL-6 or 100 ng/mL anti-TNF- $\alpha$ . ER $\alpha$  transactivation was measured with the ONE-Glo assay. Monocultures exposed to neutralizing antibodies served as negative controls.

### Statistical Analyses

Data sets were analyzed with GraphPad Prism 9.4.1. Unless otherwise stated, each data set represents the average and standard deviation of measurements collected from three cell passages. Statistically significant differences (\*) correspond to a *p*-value of  $\leq 0.05$ .

## EXPERIMENTAL DESIGN

Paper is a readily available material capable of supporting cell-laden hydrogels in a 3D environment. The volume of these cell-containing regions is defined by the thickness of the paper, its porosity, and a wax-printed border. Wax printing accommodates user-defined scaffold sizes and shapes to meet experimental or analysis requirements.<sup>34,35</sup> A benefit of the wax borders is their buoyancy, ensuring the cell-laden scaffold remains at the air–liquid interface throughout an experiment. Figure 1 outlines the three culture configurations used in this work, each representing different aspects of the breast tumor microenvironment during luminal cancer development. The schematics represent the cross-section of a healthy lumen in which a proteinaceous basement membrane separates the epithelial cells lining the inside of the duct from the stromal components. For simplicity, we focus on only fibroblasts but acknowledge that there are many cell types present in the stroma. A cancer-initiating event causes one or multiple

epithelial cells to disregard homeostatic signals and proliferate rapidly. The continued division of these cancerous cells results in a tumor mass within the lumen, a so-called ductal carcinoma in situ (DCIS). The tumor can progress further and, with the help of fibroblasts, degrade the basement membrane. The compromised barrier allows tumorigenic cells to invade the neighboring stroma and fibroblasts to enter the tumor to repair the tissue. The missing basement membrane and intermingling of cell types is known as an invasive ductal carcinoma (IDC).

To mimic the solid tumor environment, we deposited breast cancer cells suspended in a collagen I matrix into the paper scaffolds. The cell-laden collagen was prepared by resuspending a known number of cells in a centrifuged pellet into a neutralized collagen I matrix. While solubilized basement membrane protein extracts are a commonly used in breast duct models,<sup>36</sup> we chose collagen because it is less likely to contain estrogenic molecules that could interfere with hormone signaling. We focused on the ER+T47D and MCF7 cell lines because they stably express ER $\alpha$ . The triple negative M231 cell line served as a control, accounting for non-ER $\alpha$  cellular changes caused by the fibroblasts or other experimental conditions. We chose normal-associated or lobular mammary fibroblasts because they are the most abundant cell type in healthy breast tissue and an important regulator of both the healthy tissue and tumor environment.<sup>37,38</sup>

The monoculture configuration (Figure 1D) contained only breast cancer cells and served as a quantitative benchmark for the cellular responses to E2 in the absence of intercellular signaling. In this configuration, the breast cancer cell-laden paper scaffolds were placed in well plates prefilled with the culture medium. The indirect coculture configuration (Figure 1E) mimicked aspects of a DCIS, with the culture medium acting as a physical barrier separating the fibroblasts and breast cancer cell-laden paper scaffolds. To prepare these setups, fibroblasts were suspended in collagen and deposited on the bottom of a 96-well plate. The wells were filled with culture medium, and the paper scaffolds were placed in the wells. To account for the additional collagen in the indirect cocultures, we placed cell-free collagen on the bottom of the wells of the control cultures. The direct coculture configuration (Figure 1F) mimicked aspects of an IDC, with the fibroblasts and breast cancer cells suspended in the same volume of collagen and deposited into the paper scaffolds.

## RESULTS AND DISCUSSION

### Presence, Number, and Proximity of Mammary Fibroblasts Impact ER $\alpha$ Transactivation in the T47D-KBluc Cell Line

The T47D-KBluc cell line is ideal for evaluating ER $\alpha$  transactivation, as these cells are engineered with a luciferase gene downstream of three estrogen-responsive elements.<sup>39</sup> Figure 2 contains plots of luciferase activity in T47D-KBluc cells in the monoculture, indirect coculture, and direct coculture configurations after a 24 h exposure to increasing concentrations of E2 (300 fM to 1 nM). The E2 was added directly to the cell culture medium in each configuration. Background transactivation was accounted for with no-E2 (negative) control samples prepared by adding the same volume of ethanol as the dosed samples. Both luciferase activity and cell viability were measured for each experimental replicate to ensure that the changes in activity were not due to proliferation or cell death. Cell number corrections were unnecessary for this analysis, as viability measures were not significantly different across the range of E2 concentrations tested according to a one-way analysis of variance (ANOVA) of the log-transformed data sets. Following the procedures detailed in earlier studies,<sup>40</sup> the percent luciferase activity relative to the maximal signal was plotted and fit with a four-parameter logistic. The maximum signal referenced was from monocultures after a 24 h exposure to 10 nM E2. These fits provided estimates of the E2 potency and transactivation

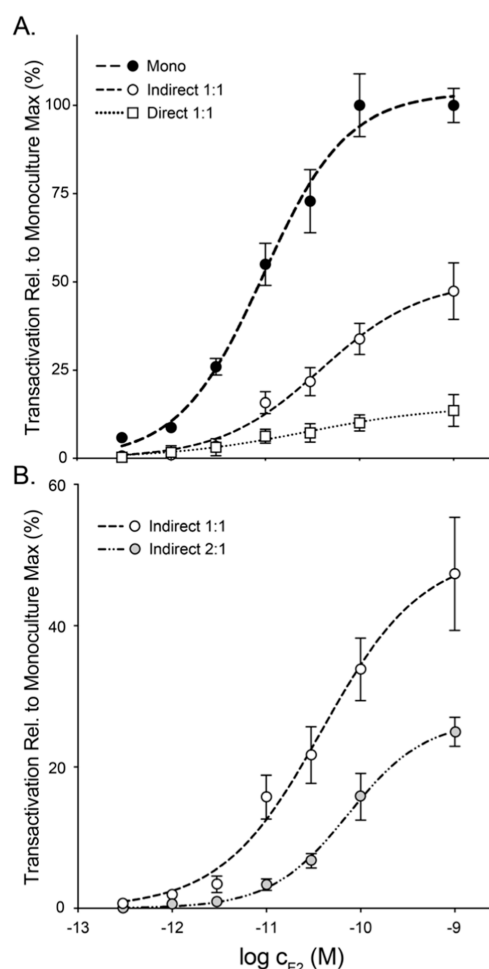


**Figure 2.** ER $\alpha$  transactivation in  $4.0 \times 10^4$  T47D-KBluc cells suspended in collagen. The cell-laden collagen suspension was deposited in paper scaffolds and luciferase activity measured after a 24 h exposure to E2. (A) Monoculture, indirect, and direct coculture configurations containing equal numbers of fibroblasts and cancer cells (1:1). (B) Indirect coculture configurations containing an equal number of fibroblasts (1:1) or  $8.0 \times 10^4$  fibroblasts (2:1). Each data point is the average and standard deviation of at least 10 separate cultures prepared from at least 2 cell passages. The data sets are plotted as the percentage of the maximal response obtained from a monoculture dosed with 10 nM E2. The dashed lines correspond to a four-parameter logistic fit.

magnitude for each culture configuration. Potency ( $EC_{50}$ ) values correspond to the E2 concentration needed to elicit half the maximum luciferase activity. For ease of comparison, we calculated a monoculture equivalency (ME) (eq 1) value. The magnitude of transactivation is the maximum difference in the luciferase activity for the E2 concentrations evaluated. These values are summarized in Table 1.

$$ME = \frac{EC_{50, \text{coculture}}}{EC_{50, \text{monoculture}}} \quad (1)$$

Figure 2A contains the data sets comparing ER $\alpha$  transactivation in paper scaffolds containing  $4.0 \times 10^4$  T47D-KBluc cells. The coculture configurations contained an equal number of RMFs. The addition of fibroblasts decreased estrogen responsiveness significantly compared to the monoculture configuration, as determined with an extra-sum-of-squares F-test. The difference in  $EC_{50}$  values for the indirect and direct

**Table 1. Summary of ER $\alpha$  Transactivation Data Sets**

culture configuration	RMF-to-T47D-KBluc ratio	EC <sub>50</sub> value (M)	ME value	span (%)
monoculture		$9.5 \times 10^{-12}$ *	1.0	103.7
indirect	1:1	$3.9 \times 10^{-11a}$	4.1	50.4 <sup>a,b</sup>
	2:1	$7.4 \times 10^{-11a}$	7.8	26.7 <sup>a,b</sup>
direct	1:1	$2.7 \times 10^{-11a}$	2.8	15.0 <sup>a,b</sup>
	2:1	$5.8 \times 10^{-11a}$	6.1	5.5 <sup>a,b</sup>

<sup>a</sup>Indicates statistically significant difference from the monoculture.

<sup>b</sup>Indicates statistically significant differences between each indicated coculture configuration.

coculture configurations was not statistically significant. Rationalizing the molecular mechanism of these potency changes is difficult, given the multiple steps between E2 binding and luciferase expression and folding. We note that similar observations were made by Beebe, as E2 potency in MCF7 cells decreased 2.7-fold in the presence of fibroblasts.<sup>41</sup> Comparisons of transactivation magnitude indicate the presence and proximity of the fibroblasts affect ER $\alpha$  activity levels while not altering the binding affinity for E2 (i.e., similar EC<sub>50</sub> values). The large decrease in ER $\alpha$  activity in the indirect (50%) and direct (94%) cocultures compared to the monoculture configuration suggest a concentration-dependent response. To test this hypothesis, we compared ER $\alpha$  transactivation in the presence of an increasing number of fibroblasts. Figure 2B is a plot of transactivation the indirect coculture configurations containing  $4.0 \times 10^4$  T47D-KBluc cells and a 1:1 or 2:1 RMF-to-T47D-KBluc ratio. Figure S2 is the corresponding data set for the direct coculture configuration. The changes in E2 potency for an increasing fibroblast number were not statistically significant. The decreased activity in the presence of double the fibroblasts for each coculture configuration further suggests a concentration-dependent response from a stromal signaling factor.

### Mammary Fibroblasts Inhibit E2-Promoted Growth in ER+ Cells

Another consequence of estrogen signaling in breast cancer is the enhanced proliferation of ER+ cells. To determine if the RMFs were inhibiting other aspects of cellular responses to E2/ER $\alpha$  transactivation, we measured changes in cell number after a 7 day exposure to different combinations of E2 and the selective estrogen receptor modulator, tamoxifen (TAM). TAM is a commonly used adjuvant hormone therapy in ER+

breast cancer patients. Its mechanism of action is antagonistic, binding to ER $\alpha$  with a higher affinity than E2 and preventing hormone-mediated activation of the receptor.<sup>42</sup>

In this experimental setup, paper scaffolds containing  $2.0 \times 10^3$  breast cancer cells suspended in collagen were placed in a 96-well plate containing 200  $\mu$ L of culture medium. Half of the medium was replaced every 48 h throughout the experiment. In the indirect coculture setup, the bottom of each well contained  $4.0 \times 10^4$  RMFs suspended in collagen. We chose this number of fibroblasts to match the previous experimental setups with the rationale that an excess of fibroblasts is physiologically relevant for tumor initiation. Figure 3 contains a plot that summarizes the relative fold-change of the T47D, MCF7, or M231 cells in both the monoculture and indirect coculture configurations. In the monocultures, 10 nM E2 increased the proliferation of the ER+ MCF7 and T47D cells by approximately 2-fold compared with their hormone-starved counterparts. The presence of E2 did not affect the M231 cells, which served as an experimental control, given their lack of ER $\alpha$  expression. The addition of 1  $\mu$ M TAM decreased the proliferation in all three cell lines. This decrease was expected for the ER+ cell lines, given the drug's mechanism of action. The decreased proliferation of the M231 cells was surprising to us, but Sutherland showed sublethal doses of TAM inhibit proliferation in ER+ and ER- cells.<sup>43</sup> These low doses of tamoxifen have a proapoptotic effect, initiated by increased calcium influx.<sup>42</sup>

The RMFs inhibited any E2-induced proliferation of the T47D or MCF7 cells. A comparison of the proliferation in the presence of E2 and TAM in both the mono- and coculture configurations suggests that the TAM is responsible for the decreased proliferation. Kabos also found E2 did not increase the proliferation of MCF7 cells cocultured with normal-associated fibroblasts.<sup>44</sup> However, these studies found that the fibroblasts abrogated the effects of TAM compared with MCF7 monocultures. Three experimental variables could account for the differences observed in between our study and these previous results studies: TAM concentration (100 nM vs our 1  $\mu$ M), duration (5 days vs our 7 days), and the inclusion of an ECM (collagen vs none).

### Mammary Fibroblasts Do Not Alter ER $\alpha$ Expression Levels or Decrease Its Transcriptional Activity

To determine if the fibroblasts affected ER $\alpha$  regulation at the receptor level, we quantified protein levels with an ELISA and

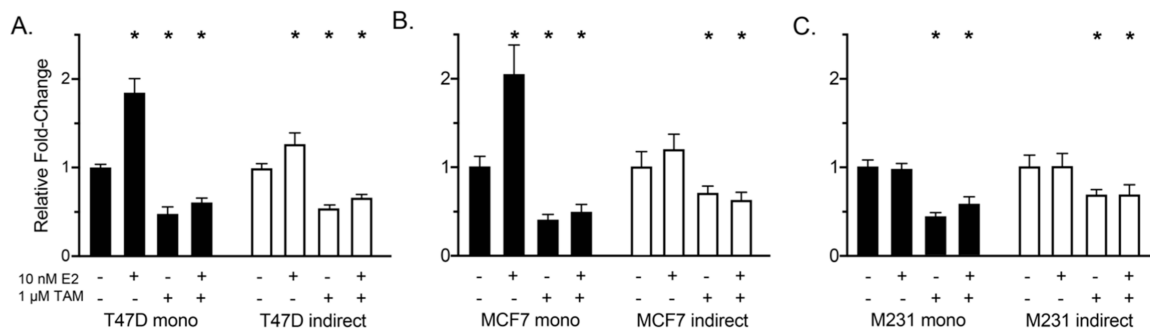


**Figure 3.** Fold-changes of (A) T47D, (B) MCF7, and (C) M231 cells relative to a vehicle control after a 7-d exposure to different combinations of E2 and TAM. The paper scaffolds contained  $2.0 \times 10^3$  breast cancer cells suspended in collagen; the indirect coculture configurations contained  $4.0 \times 10^4$  RMFs suspended in collagen, which were precoated on the bottom of a well plate. Each bar represents the average and standard error of the mean (SEM) of at least 5 replicates from 2 cell passages. \* denotes  $p < 0.05$  from the vehicle control, determined with a one-way ANOVA and assuming unequal standard deviations between data sets.

transcriptional activity with real-time quantitative reverse transcription PCR (RT-qPCR). Figure 4A is a plot of ER $\alpha$

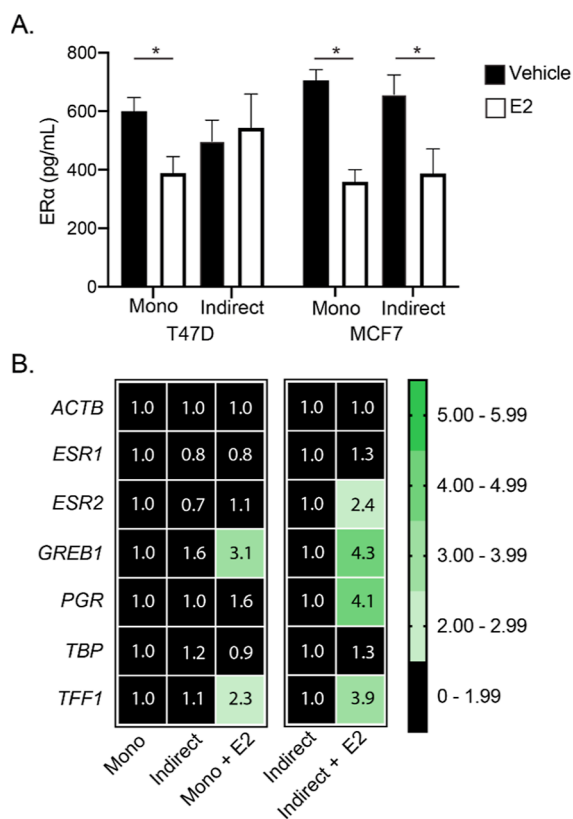


**Figure 4.** Transcript and protein-level changes when monoculture and indirect coculture configurations were exposed to E2 for 24 h. Paper scaffolds were deposited with  $4.0 \times 10^4$  T47D or MCF7 cells suspended in collagen. The indirect cocultures contained an equal number of RMFs suspended in collagen. Each value represents at least 4 separate setups prepared from at least 2 cell passages. (A) ER $\alpha$  protein levels in the T47D and MCF7 cells were determined with an ELISA. (B) Transcript-level changes for T47D cells were determined with RT-qPCR and the  $\Delta\Delta\text{Ct}$  method, using *ACTB* as the housekeeping gene. \* denotes  $p < 0.05$  for protein concentration measurements, determined with a Student's *t*-test and Welch's correction. A transcript fold change of greater than two, that was statistically significant with a Student's *t*-test, was considered biologically significant (green in color).

levels in the T47D and MCF7 cells in the presence of E2 or a vehicle control. The addition of 10 nM E2 significantly decreased protein levels in the monoculture configuration: a 1.5-fold decrease in the T47D cells and a 1.8-fold decrease in the MCF7 cells. This decrease was expected, as the activation and translocation of ER $\alpha$  decreases its half-life in the cell from 5 d to 3 h.<sup>45</sup> The inclusion of an equal number of fibroblasts in the indirect coculture configurations did not affect the basal levels of ER $\alpha$  in either cell line. The addition of E2 decreased ER $\alpha$  levels by 1.8-fold in the MCF7 cells but did not affect protein levels in the T47D cells. The unchanged protein levels in T47D could result from delayed receptor degradation, although further studies are needed to determine the exact mechanism for this response.

Figure 4B is a heatmap of estrogen-sensitive and insensitive genes quantified in the T47D cell line in the monoculture and indirect coculture configurations. Figure S3 is the analogous heatmap for the MCF7 cell line. The relative changes in

expression were determined with the  $\Delta\Delta\text{Ct}$  method,<sup>32</sup> with *ACTB* serving as the housekeeping gene. A fold change of greater than two and statistically significant with a Student's *t*-test was considered biologically significant. The estrogen-sensitive genes included growth-regulating estrogen binding 1 protein (*GREB1*), progesterone receptor (*PGR*), and trefoil factor 1 (*TFF1*). The estrogen-insensitive gene was the TATA-binding protein (*TBP*), a component of the RNA polymerase complex. We also quantified ER $\alpha$  (*ESR1*) and estrogen receptor beta (*ER $\beta$* , *ESR2*). In the monocultures, E2 increased transcript profiles that matched previous studies.<sup>46,47</sup> The T47D cells had increased levels of *TFF1* and *GREB1* while only *PGR* increased significantly in the MCF7 cells. These differences in expression profiles between the two lines are likely a result of their different ER $\alpha$ /ER $\beta$  ratios,<sup>48</sup> as both the receptors are activated by E2 but target different genes.

The fibroblasts did not affect the basal levels of these four genes in either the MCF7 or T47D cells. In the T47D cells, the combination of fibroblasts and E2 significantly increased *GREB1*, *PGR*, and *TFF1* levels. These data suggest that the decreased luciferase activity observed in the transactivation assays was due to a decrease at the protein level, likely through modulated activity, as the expression levels of ER $\alpha$  were unchanged between the monoculture and indirect coculture configurations (Figure 4A). Another possibility for these changes in expression could be an increased expression and activity of ER $\beta$  when T47D cells are exposed to E2, as the transcript of *ESR2* is unchanged by the fibroblasts but significantly increased by fibroblasts and E2. We are unaware of the studies that have looked at this interplay of receptors in these types of culture configurations, something we believe merits further investigation.

#### Fibroblast-Secreted IL-6 Regulates Estrogen Sensitivity in the T47D Cells

We hypothesized that intercellular signaling was responsible for the decreased E2 sensitivity in ER+ breast cancer cells. Signaling between the developing tumor and the stroma plays an important role in cancer progression. To determine which signaling molecules secreted by the fibroblasts decreased luciferase activity in the T47D-KBluc cells, we screened IL-6, IL-8, SDF-1, and TGF- $\beta$ . IL-6 stimulates growth and invasiveness in MCF7 cells and is correlated with TAM resistance.<sup>49,50</sup> IL-8 is an angiogenic stimulator but does not affect ER $\alpha$  signaling.<sup>51,52</sup> TGF- $\beta$  restricts ER $\alpha$ -mediated cell proliferation and the likely transactivation of ER-regulated genes.<sup>53</sup> SDF-1 is proangiogenic and results in ligand-independent ER $\alpha$  signaling by phosphorylating the receptor.<sup>54,55</sup> We screened a fifth signaling molecule, which served as a negative control that should not be present in the coculture configurations. TNF- $\alpha$  was selected because it is an inflammatory marker secreted by macrophages and has known crosstalk with the ER $\alpha$  pathway.<sup>56</sup>

First, we screened human recombinant proteins of these five factors by adding them to T47D-KBluc monocultures. Cell-containing paper scaffolds were placed in the wells of a 96-well plate containing 200  $\mu\text{L}$  of culture medium with one of the four combinations: (1) 10 nM E2 plus 100 ng/mL of signaling molecule, (2) 10 nM E2 plus a vehicle control for the signaling molecule, (3) a vehicle control for E2 plus 100 ng/mL of signaling molecule, and (4) vehicle control for both E2 and the signaling molecule. The first combination represented the condition of interest and is plotted in Figure 5A after

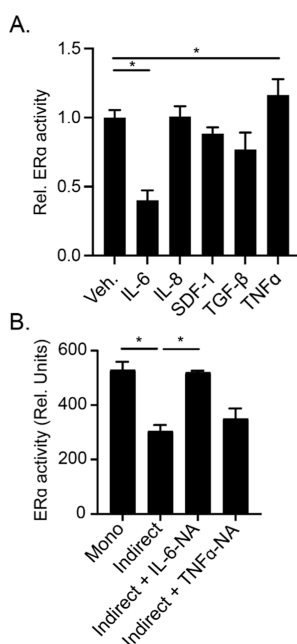


**Figure 5.** (A) ER $\alpha$  transactivation in monocultures of  $4.0 \times 10^4$  T47D-KBluc cells exposed to 10 nM E2 and 100 ng/mL of the signaling molecule for 24 h. Each value is relative to a vehicle control (Veh.) in which the cells were exposed to 1X DPBS (Dulbecco's phosphate buffered saline). (B) ER $\alpha$  transactivation in the indirect coculture configuration containing equal numbers of T47D-KBluc cells and RMFs. The cells were exposed to 10 nM E2 and 800 ng/mL IL-6 or 100 ng/mL of TNF- $\alpha$  neutralizing antibodies for 24 h. The monoculture (Mono) and indirect controls were exposed to 1X DPBS. Each bar represents (A) at least 4 replicate cultures prepared from 2 cell passages or (B) at least 8 replicate cultures prepared from 2 cell passages. \* denotes  $p < 0.05$ , determined with a  $t$ -test with Welch's correction.

background correction. The second combination ensured that the T47D-KBluc cells responded as expected to E2. The third combination accounted for any changes in basal ER $\alpha$  transactivation caused by the signaling molecule. The fourth combination served as the background or basal ER $\alpha$  transactivation occurring in the monoculture format.

Figure 5A is a plot of background-corrected luciferase activity for each signaling molecule after a 24 h incubation. Two factors significantly differed from the positive control, which contained 10 nM : IL-6 decreased activity by 60% and TNF- $\alpha$  increased activity by 16%. To confirm their role in altering estrogen sensitivity in the indirect cocultures, we compared ER $\alpha$  transactivation after a 24 h exposure to 10 nM E2 and either TNF- $\alpha$ -neutralizing antibodies (100 ng/mL) or IL-6-neutralizing antibodies (800 ng/mL). Figure 5B summarizes the results of the neutralizing antibody experiments. The TNF- $\alpha$ -neutralizing antibodies did not recover ER $\alpha$  signaling, with luciferase activities matching the indirect cocultures. This result was expected, as TNF- $\alpha$  was not present in this configuration. The transactivation levels in the monoculture and coculture containing IL-6 neutralizing antibodies were equivalent, confirming IL-6 plays an important role in modulating estrogen responsiveness. IL-6 is known to drive breast cancer through non-ER $\alpha$  mechanisms in combination with signal transducer and activator of transcription 3 (STAT3).<sup>57</sup> Its role in ER $\alpha$ -mediated signaling is unexplored as far as we can tell.

## CONCLUSIONS

Tissue-like cultures are necessary to evaluate the hormone signaling and drug sensitivity of tumor cells at different stages of breast cancer progression. Extracellular matrices and stromal components are integral parts of the tumor microenvironment, which impact cellular phenotypes and responses that cannot be found in the traditionally relied upon monolayer cultures. Using paper-based scaffolds, we further highlight the utility of this culture platform to rapidly prototype new culture configurations. Specifically, we probed the effect of fibroblast presence, number, and proximity on estrogen sensitivity and ER $\alpha$  transactivation in ER+ breast cancer lines. Through a systematic evaluation of breast cancer cell responses in the presence and absence of normal fibroblasts, we determined that decreased cellular sensitivity in the T47D cell line was inversely related to the RMF proximity. This decreased level of ER $\alpha$  transactivation was mitigated by the addition of neutralizing antibodies against IL-6, highlighting its role in estrogen signaling. While these results demonstrate the importance of paracrine signaling in modulating estrogen sensitivity in ER+ tumors, they prompt many questions about the molecular-level regulation occurring in these systems. These results highlight the ability of the paper-based cultures to perform detailed studies of hormone receptor function and regulation, supporting their further use in screening the effects of paracrine signaling dynamics with fibroblasts and other stromal components.

## ASSOCIATED CONTENT

### Supporting Information

The Supporting Information is available free of charge at <https://pubs.acs.org/doi/10.1021/acsmesuresciau.3c00032>.

Photographs of paper scaffolds, RT-qPCR sequences and optimized amplification conditions, dose-response curves for the direct coculture configurations, and RT-qPCR data sets for the MCF7 cell line (PDF)

## AUTHOR INFORMATION

### Corresponding Author

**Matthew R. Lockett** – Department of Chemistry, University of North Carolina at Chapel Hill, Chapel Hill, North Carolina 27599-3290, United States; Lineberger Comprehensive Cancer Center, University of North Carolina at Chapel Hill, Chapel Hill, North Carolina 27599-7295, United States; [orcid.org/0000-0003-4851-7757](https://orcid.org/0000-0003-4851-7757); Email: [mlockett@unc.edu](mailto:mlockett@unc.edu)

### Authors

**Zachary R. Sitte** – Department of Chemistry, University of North Carolina at Chapel Hill, Chapel Hill, North Carolina 27599-3290, United States

**Abel Andre Miranda Buzetta** – Department of Chemistry, University of North Carolina at Chapel Hill, Chapel Hill, North Carolina 27599-3290, United States

**Sarina J. Jones** – Department of Chemistry, University of North Carolina at Chapel Hill, Chapel Hill, North Carolina 27599-3290, United States

**Zhi-Wei Lin** – Department of Chemistry, University of North Carolina at Chapel Hill, Chapel Hill, North Carolina 27599-3290, United States

Nathan Ashbrook Whitman – Department of Chemistry,  
University of North Carolina at Chapel Hill, Chapel Hill,  
North Carolina 27599-3290, United States

Complete contact information is available at:

<https://pubs.acs.org/10.1021/acsmeasuresciau.3c00032>

### Author Contributions

§Z.R.S., A.A.M.B., and S.J.J. indicate coauthorship. CRediT: Zachary R Sitte conceptualization, investigation, methodology, validation, writing-original draft, writing-review & editing; Abel Andre Miranda Buzetta conceptualization, formal analysis, investigation, methodology, validation, writing-original draft, writing-review & editing; Sarina J. Jones investigation, methodology, validation, writing-original draft, writing-review & editing; Zhi-Wei Lin conceptualization, investigation, methodology, writing-original draft; Nathan Ashbrook Whitman conceptualization, investigation, methodology, writing-original draft; Matthew R. Lockett conceptualization, funding acquisition, project administration, supervision, writing-original draft, writing-review & editing.

### Notes

The authors declare no competing financial interest.

### ACKNOWLEDGMENTS

This work was supported by funding provided by the National Institute of General Medical Sciences through Grant Award Number R35 GM128697. We thank Dr. Thomas DiProspero for helpful conversations and obtaining initial RT-qPCR data sets.

### REFERENCES

- (1) Siegel, R. L.; Miller, K. D.; Fuchs, H. E.; Jemal, A. Cancer statistics, 2022. *Ca-Cancer J. Clin.* **2022**, *72* (1), 7–33.
- (2) Cancer Facts & Figures 2022, 2022. <http://cancerstatisticscenter.cancer.org> (accessed March, 2023).
- (3) Rakha, E. A.; Tse, G. M.; Quinn, C. M. An update on the pathological classification of breast cancer. *Histopathology* **2023**, *82* (1), 5–16.
- (4) Bouris, P.; Skandalis, S. S.; Piperigkou, Z.; Afratis, N.; Karamanou, K.; Aletras, A. J.; Moustakas, A.; Theocharis, A. D.; Karamanos, N. K. Estrogen receptor alpha mediates epithelial to mesenchymal transition, expression of specific matrix effectors and functional properties of breast cancer cells. *Matrix Biol.* **2015**, *43* (1), 42–60.
- (5) Thomas, C.; Gustafsson, J. A. The different roles of ER subtypes in cancer biology and therapy. *Nat. Rev. Cancer* **2011**, *11* (8), 597–608.
- (6) Burstein, H. J.; Lacchetti, C.; Anderson, H.; Buchholz, T. A.; Davidson, N. E.; Gelmon, K. A.; Giordano, S. H.; Hudis, C. A.; Solky, A. J.; Stearns, V.; et al. Adjuvant endocrine therapy for women with hormone receptor-positive breast cancer: ASCO clinical practice guideline focused update. *J. Clin. Oncol.* **2019**, *37* (5), 423–438.
- (7) Osborne, C. K.; Schiff, R. Mechanisms of endocrine resistance in breast cancer. *Annu. Rev. Med.* **2011**, *62* (1), 233–247.
- (8) de Leeuw, R.; Neeffes, J.; Michalides, R. A role for estrogen receptor phosphorylation in the resistance to tamoxifen. *Int. J. Breast Cancer* **2011**, *2011*, 1–10.
- (9) Schiff, R.; Massarweh, S.; Shou, J.; Osborne, C. K. Breast cancer endocrine resistance: How growth factor signaling and estrogen receptor coregulators modulate response. *Clin. Cancer Res.* **2003**, *9* (1), 447S–454S.
- (10) Zacharewski, T. In vitro bioassays for assessing estrogenic substances. *Environ. Sci. Technol.* **1997**, *31* (3), 613–623.
- (11) Langhans, S. A. Three-dimensional in vitro cell culture models in drug discovery and drug repositioning. *Front. Pharmacol.* **2018**, *9* (1), 6.
- (12) Pampaloni, F.; Reynaud, E. G.; Stelzer, E. H. K. The third dimension bridges the gap between cell culture and live tissue. *Nat. Rev. Mol. Cell Biol.* **2007**, *8* (10), 839–845.
- (13) Hall, H. G.; Farson, D. A.; Bissell, M. J. Lumen formation by epithelial-cell lines in response to collagen overlay: A morphogenetic model in culture. *Proc. Natl. Acad. Sci. U.S.A.* **1982**, *79* (15), 4672–4676.
- (14) Wiseman, B. S.; Werb, Z. Stromal effects on mammary gland development and breast cancer. *Science* **2002**, *296* (5570), 1046–1049.
- (15) Avagliano, A.; Fiume, G.; Ruocco, M. R.; Martucci, N.; Vecchio, E.; Insabato, L.; Russo, D.; Accurso, A.; Masone, S.; Montagnani, S.; et al. Influence of fibroblasts on mammary gland development, breast cancer microenvironment remodeling, and cancer cell dissemination. *Cancers* **2020**, *12* (6), 1697.
- (16) Alkasalias, T.; Moyano-Galceran, L.; Arsenian-Henriksson, M.; Lehti, K. Fibroblasts in the tumor microenvironment: Shield or spear? *Int. J. Mol. Sci.* **2018**, *19* (5), 1532.
- (17) Frohlich, E. The variety of 3D breast cancer models for the study of tumor physiology and drug screening. *Int. J. Mol. Sci.* **2023**, *24* (8), 7116.
- (18) Shaw, F. L.; Harrison, H.; Spence, K.; Ablett, M. P.; Simoes, B. M.; Farnie, G.; Clarke, R. B. A detailed mammosphere assay protocol for the quantification of breast stem cell activity. *J. Mammary Gland Biol. Neoplasia.* **2012**, *17* (2), 111–117.
- (19) Brock, E. J.; Ji, K.; Shah, S.; Mattingly, R. R.; Sloane, B. F. In vitro models for studying invasive transitions of ductal carcinoma in situ. *J. Mammary Gland Biol. Neoplasia.* **2019**, *24* (1), 1–15.
- (20) Derda, R.; Laromaine, A.; Mammoto, A.; Tang, S. K.; Mammoto, T.; Ingber, D. E.; Whitesides, G. M. Paper-supported 3D cell culture for tissue-based bioassays. *Proc. Natl. Acad. Sci. U.S.A.* **2009**, *106* (44), 18457–18462.
- (21) Kenney, R. M.; Lee, M. C.; Boyce, M. W.; Sitte, Z. R.; Lockett, M. R. Cellular Invasion Assay for the Real-Time Tracking of Individual Cells in Spheroid or Tumor-like Mimics. *Anal. Chem.* **2023**, *95* (5), 3054–3061.
- (22) Kenney, R. M.; Loeser, A.; Whitman, N. A.; Lockett, M. R. Paper-based Transwell assays: An inexpensive alternative to study cellular invasion. *Analyst* **2019**, *144* (1), 206–211.
- (23) Truong, A. S.; Lochbaum, C. A.; Boyce, M. W.; Lockett, M. R. Tracking the invasion of small numbers of cells in paper-based assays with quantitative PCR. *Anal. Chem.* **2015**, *87* (22), 11263–11270.
- (24) Whitman, N. A.; Lin, Z. W.; DiProspero, T. J.; McIntosh, J. C.; Lockett, M. R. Screening estrogen receptor modulators in a paper-based breast cancer model. *Anal. Chem.* **2018**, *90* (20), 11981–11988.
- (25) Whitman, N.; Lin, Z.; Kenney, R.; Albertini, L.; Lockett, M. Hypoxia differentially regulates estrogen receptor alpha in 2D and 3D culture formats. *Arch. Biochem. Biophys.* **2019**, *671* (1), 8–17.
- (26) Boyce, M.; LaBonia, G.; Hummon, A.; Lockett, M. Assessing chemotherapeutic effectiveness using a paper-based tumor model. *Analyst* **2017**, *142* (15), 2819–2827.
- (27) Larson, T.; Glish, G.; Lockett, M. Spatially resolved quantification of drug metabolism and efficacy in 3D paper-based tumor mimics. *Anal. Chim. Acta* **2021**, *1186*, 339091.
- (28) Kuperwasser, C.; Chavarria, T.; Wu, M.; Magrane, G.; Gray, J. W.; Carey, L.; Richardson, A.; Weinberg, R. A. Reconstruction of functionally normal and malignant human breast tissues in mice. *Proc. Natl. Acad. Sci. U.S.A.* **2004**, *101* (14), 4966–4971.
- (29) Camp, J. T.; Elloumi, F.; Roman-Perez, E.; Rein, J.; Stewart, D. A.; Harrell, J. C.; Perou, C. M.; Troester, M. A. Interactions with fibroblasts are distinct in basal-like and luminal breast cancers. *Mol. Cancer Res.* **2011**, *9* (1), 3–13.
- (30) Lloyd, C.; Boyce, M.; Lockett, M. Paper-based invasion assays for quantifying cellular movement in three-dimensional tissue-like structures. *Curr. Protoc. Chem. Biol.* **2017**, *9* (2), 75–95.

- (31) Sitte, Z. R.; DiProspero, T. J.; Lockett, M. R. Evaluating the impact of physiologically relevant oxygen tensions on drug metabolism in 3D hepatocyte cultures in paper scaffolds. *Curr. Protoc.* **2023**, *3* (2), No. e662.
- (32) Livak, K. J.; Schmittgen, T. D. Analysis of Relative Gene Expression Data Using Real-Time Quantitative PCR and the  $2^{-\Delta\Delta CT}$  Method. *Methods* **2001**, *25* (4), 402–408.
- (33) Karlen, Y.; McNair, A.; Perseguers, S.; Mazza, C.; Mermod, N. Statistical significance of quantitative PCR. *BMC Bioinf.* **2007**, *8* (1), 131.
- (34) Cramer, S. M.; Larson, T. S.; Lockett, M. R. Tissue Papers: Leveraging paper-based microfluidics for the next generation of 3D tissue models. *Anal. Chem.* **2019**, *91* (17), 10916–10926.
- (35) Ng, K.; Gao, B.; Yong, K. W.; Li, Y. H.; Shi, M.; Zhao, X.; Li, Z. D.; Zhang, X. H.; Pingguan-Murphy, B.; Yang, H.; et al. Paper-based cell culture platform and its emerging biomedical applications. *Mater. Today* **2017**, *20* (1), 32–44.
- (36) Shaw, K. R. M.; Wrobel, C. N.; Brugge, J. S. Use of Three-Dimensional Basement Membrane Cultures to Model Oncogene-Induced Changes in Mammary Epithelial Morphogenesis. *J. Mammary Gland Biol. Neoplasia.* **2004**, *9* (4), 297–310.
- (37) Tlsty, T.; Coussens, L. Tumor stroma and regulation of cancer development. *Annu. Rev. Pathol.* **2006**, *1*, 119–150.
- (38) Pietras, K.; Ostman, A. Hallmarks of cancer: Interactions with the tumor stroma. *Exp. Cell Res.* **2010**, *316* (8), 1324–1331.
- (39) Wilson, V. S.; Bobseine, K.; Gray, L. E. Development and characterization of a cell line that stably expresses an estrogen-responsive luciferase reporter for the detection of estrogen receptor agonist and antagonists. *Toxicol. Sci.* **2004**, *81* (1), 69–77.
- (40) Conley, J. M.; Hannas, B. R.; Furr, J. R.; Wilson, V. S.; Gray, L. E. A demonstration of the uncertainty in predicting the estrogenic activity of individual chemicals and mixtures from an in vitro estrogen receptor transcriptional activation assay (T47D-KBluc) to the in vivo uterotrophic assay using oral exposure. *Toxicol. Sci.* **2016**, *153* (2), 382–395.
- (41) Morgan, M.; Livingston, M.; Warrick, J.; Stanek, E.; Alarid, E.; Beebe, D.; Johnson, B. Mammary fibroblasts reduce apoptosis and speed estrogen-induced hyperplasia in an organotypic MCF7-derived duct model. *Sci. Rep.* **2018**, *8* (1), 7139.
- (42) Radin, D. P.; Patel, P. Delineating the molecular mechanisms of tamoxifen's oncolytic actions in estrogen receptor-negative cancers. *Eur. J. Pharmacol.* **2016**, *781*, 173–180.
- (43) Reddel, R.; Murphy, L.; Hall, R.; Sutherland, R. Differential sensitivity of human breast cancer cell lines to the growth inhibitory effects of tamoxifen. *Cancer Res.* **1985**, *45* (4), 1525–1531.
- (44) Brechbuhl, H. M.; Finlay-Schultz, J.; Yamamoto, T. M.; Gillen, A. E.; Cittelly, D. M.; Tan, A. C.; Sams, S. B.; Pillai, M. M.; Elias, A. D.; Robinson, W. A.; et al. Fibroblast subtypes regulate responsiveness of luminal breast cancer to estrogen. *Clin. Cancer Res.* **2017**, *23* (7), 1710–1721.
- (45) Nawaz, Z.; Lonard, D.; Dennis, A.; Smith, C.; O'Malley, B. Proteasome-dependent degradation of the human estrogen receptor. *Proc. Natl. Acad. Sci. U.S.A.* **1999**, *96* (5), 1858–1862.
- (46) Williams, C.; Edvardsson, K.; Lewandowski, S.; Strom, A.; Gustafsson, J. A genome-wide study of the repressive effects of estrogen receptor beta on estrogen receptor alpha signaling in breast cancer cells. *Oncogene* **2008**, *27* (7), 1019–1032.
- (47) Rangel, N.; Villegas, V. E.; Rondon-Lagos, M. Profiling of gene expression regulated by  $17\beta$ -estradiol and tamoxifen in estrogen receptor-positive and estrogen receptor-negative human breast cancer cell lines. *Breast Cancer* **2017**, *9*, 537–550.
- (48) Buterin, T.; Koch, C.; Naegeli, H. Convergent transcriptional profiles induced by endogenous estrogen and distinct xenoestrogens in breast cancer cells. *Carcinogenesis* **2005**, *27* (8), 1567–1578.
- (49) Studebaker, A. W.; Storci, G.; Werbeck, J. L.; Sansone, P.; Sasser, A. K.; Tavolari, S.; Huang, T.; Chan, M. W. Y.; Marini, F. C.; Rosol, T. J.; et al. Fibroblasts isolated from common sites of breast cancer metastasis enhance cancer cell growth rates and invasiveness in an interleukin-6-dependent manner. *Cancer Res.* **2008**, *68* (21), 9087–9095.
- (50) Tsoi, H.; Man, E. P. S.; Chau, K. M.; Khoo, U. S. Targeting the IL-6/STAT3 signalling cascade to reverse tamoxifen resistance in estrogen receptor positive breast cancer. *Cancers* **2021**, *13* (7), 1511.
- (51) Todorovic-Rakovic, N.; Milovanovic, J. Interleukin-8 in Breast Cancer Progression. *J. Interferon Cytokine Res.* **2013**, *33* (10), 563–570.
- (52) Freund, A.; Chauveau, C.; Brouillet, J. P.; Lucas, A.; Lacroix, M.; Licznar, A.; Vignon, F.; Lazennec, G. IL-8 expression and its possible relationship with estrogen-receptor-negative status of breast cancer cells. *Oncogene* **2003**, *22* (2), 256–265.
- (53) Band, A. M.; Laiho, M. Crosstalk of TGF- $\beta$  and estrogen receptor signaling in breast cancer. *J. Mammary Gland Biol. Neoplasia.* **2011**, *16* (2), 109–115.
- (54) Rhodes, L. V.; Bratton, M. R.; Zhu, Y.; Tilghman, S. L.; Muir, S. E.; Salvo, V. A.; Tate, C. R.; Elliott, S.; Nephew, K. P.; Collins-Burow, B. M.; et al. Effects of SDF-1–CXCR4 signaling on microRNA expression and tumorigenesis in estrogen receptor- $\alpha$  (ER- $\alpha$ )-positive breast cancer cells. *Exp. Cell Res.* **2011**, *317* (18), 2573–2581.
- (55) Kang, H.; Watkins, G.; Parr, C.; Douglas-Jones, A.; Mansel, R. E.; Jiang, W. G. Stromal cell derived factor-1: Its influence on invasiveness and migration of breast cancer cells in vitro, and its association with prognosis and survival in human breast cancer. *Breast Cancer Res.* **2005**, *7* (4), R402–R410.
- (56) Frasar, J.; Weaver, A.; Pradhan, M.; Dai, Y.; Miller, L. D.; Lin, C. Y.; Stanculescu, A. Positive crosstalk between estrogen receptor and NF- $\kappa$ B in breast cancer. *Cancer Res.* **2009**, *69* (23), 8918–8925.
- (57) Siersbaek, R.; Scabia, V.; Nagarajan, S.; Chernukhin, I.; Papachristou, E. K.; Broome, R.; Johnston, S. J.; Joosten, S. E. P.; Green, A. R.; Kumar, S.; et al. IL6/STAT3 Signaling Hijacks Estrogen Receptor  $\alpha$  Enhancers to Drive Breast Cancer Metastasis. *Cancer Cell* **2020**, *38* (3), 412–423.e9.